J. COMBIN. MATH. COMBIN. COMPUT. 127a (2025) 7493--7514

Journal of Combinatorial Mathematics and Combinatorial Computing
www.combinatorialpress.com/jcmcc

Path Selection and Congestion Mitigation Strategies Based on Deep Learning and Traffic Simulation Models

Yuance Yang[1,✉], Hongye Fan[1], Nianlu Ren[1]

[1] *School of Management and Economics, Tianjin University, Tianjin, 300072, China*

ABSTRACT

Transportation demand is gradually increasing and road traffic congestion is becoming more and more serious. Traffic state prediction is one of the important bases for accurate traffic management and control. This paper investigates a traffic state prediction method based on a deep learning algorithm fusing spatio-temporal graphical convolutional networks, and explores the law of path selection decision-making of pedestrians under different traffic flow prediction and guidance strategies, and analyzes the effect of the implementation of the information guidance policy by traffic managers in realistic scenarios using evolutionary game theory. The simulation results combined with the traffic simulation model show that the traffic state prediction method proposed in this paper is more effective compared with other models. The evolution results are more reasonable when the value of the path adjustment rate in the replicated dynamic model is the inverse of the number of iterations. In the perceptual error analysis, when the value of perceptual error θ_1 is taken to be too large, i.e., when the perceptual error of the first type of travelers is small and small, it tends to be a deterministic choice. Finally, a traffic simulation model is implemented to validate the performance of the proposed model and propose congestion mitigation strategies.

Keywords: spatio-temporal graph convolution, traffic simulation, evolutionary game, path selection

1. Introduction

Traffic congestion caused by "urbanization" and "motorization" has become an "urban disease" commonly faced by large and medium-sized cities in the world. The worsening of urban traffic and the serious problem of congestion not only bring difficulties and burdens to the residents' travel, but also cause huge economic losses, and at the same time, aggravate the urban air pollution [1-2]. With the development of sensor technology, the acquisition of traffic flow monitoring data is no longer a problem, and how to mine the operation law of road traffic system from the massive data, so as to

✉ Corresponding author.
E-mail address: nianluren@163.com (Y. Yang).
Received 25 February 2024; Revised 05 April 2024; Accepted 15 December 2024; Published Online 15 April 2025.
DOI: 10.61091/jcmcc127a-415
© 2025 The Author(s). Published by Combinatorial Press. This is an open access article under the CC BY license (https://creativecommons.org/licenses/by/4.0/).

improve the intelligent level of road traffic management, has become a research hotspot in recent years [3-6].

The core of the urban transportation system is the traveler, and the study of the traveler's behavioral patterns is an important cornerstone for conducting urban road network transportation research [7]. In-depth analysis of traveler's behavior is important for understanding and optimizing the urban transportation system. In the road transportation network, the path choice of travelers is influenced by many factors, which are closely related to individual habits and preferences, making the whole transportation system complex and dynamic [8-9]. The micro decision-making behavior of travelers determines the traffic characteristics of the macro road network [10]. The use of deep learning and other methods to describe the micro-decision-making mechanism of travelers by analyzing traffic flow monitoring data reveals the nature of the path selection process, deepens the understanding of the path selection law of travelers, and provides an effective supplement to the existing theoretical models of traffic travel analysis [11-14]. And traffic modeling and simulation is an important means to study traffic congestion characteristics and propagation laws in the field of traffic engineering, which is based on the traditional traffic flow theory [15]. The establishment of deep learning and traffic simulation model based on deep learning helps to improve the operation efficiency of road network, reduce traffic congestion, make full use of urban transportation resources, reduce vehicle emissions and energy waste, and realize the efficient and green development of urban transportation [16-19].

Influenced by personal attributes, driving style and other factors, travelers perceive the travel time difference of different paths differently, and when the difference in the utility value of changing path choice is within the tolerance interval, travelers do not change their paths, otherwise travelers will choose other paths. Based on this, many scholars have studied the effect of undifferentiated threshold on travelers' path choice behavior. Zhang, X. et al. established a structural equation model based on the Theory of Planned Behavior considering the no-difference threshold to analyze the factors affecting the degree of change in the utility of different travel behaviors of travelers, and further proposed a latent class model considering the no-difference threshold to classify them in order to propose targeted traffic management suggestions [20]. Zhang, X. et al. used an evolutionary game model based on undifferentiated thresholds to analyze travelers' path choices under changes in traffic management policies.By calculating the stable equilibrium point of the evolutionary game model, the probability of users randomly choosing their travel modes can be understood, which plays an important role in the accurate prediction of the effectiveness and stability of the implementation of traffic strategies [21]. Di, X. et al. developed a finite rational path switching model, proposed two analysis methods for the overall nondiscrepancy threshold and the mean of individual nondiscrepancy thresholds, and estimated the nondiscrepancy thresholds of travelers' travel time using empirical data [22].

In the area of traffic allocation distribution of congested road networks, scholars have likewise carried out research explorations.Menelaou, C. et al. described the road congestion problem as a mixed-integer linear programming, which utilizes heuristic algorithms to solve the proposed constraint function within a continuous-time path reservation architecture, which can have the ability to efficiently manage the vehicle path decisions, thus eliminating congested conditions [23]. Shafiei, S. et al. proposed machine learning techniques for classifying and calibrating empirical traffic data and improved simulation-based dynamic traffic assignment in conjunction with the TDOD demand estimation optimization framework, allowing it to successfully replicate traffic patterns in the network to analyze transportation operations and planning results under various conditions [24]. Saeedmanesh, M. et al. emphasized that the clustering problem of urban transportation networks is a dynamic clustering problem over time, and based on the traditional static clustering method to classify the traffic heterogeneous network, the traffic congestion problem is modeled as a mixed-integer linear optimization problem, which fully takes into account the spatio-temporal and physical properties of congestion propagation, and reclusters the traffic congestion by minimizing the heterogeneity and increasing the connectivity [25]. Although the dynamic traffic assignment linear programming model can effectively simulate typical congestion phenomena on road segments and intersections and explain congestion relief measures, the deployment of the model requires the calibration of a large number of supply and demand input parameters, and the application of deep learning algorithms is crucial.

The characteristics and interconnections of traffic flow parameters in road sections are studied and analyzed, and the collected traffic data are processed with outliers, missing values and normalization, and the data are smoothed by the design of FIR filters. Subsequently, a deep learning-based traffic flow prediction model is proposed, which employs multiple steps to construct a dynamic spatio-temporal graph and introduces a hybrid attention mechanism, effectively integrating the long- and short-term characteristics of traffic flow to improve the accuracy and reliability of traffic flow prediction. In addition, combined with the game evolution theory, the optimal selection of traffic paths is realized on the premise of traffic flow prediction. Finally, a traffic simulation model is used to realize the performance verification of the proposed model and to mine congestion relief strategies.

2. Deep learning-based traffic state prediction

2.1. Analysis of traffic flow parameters

2.1.1. Speed. Traffic flow speed can be divided into traffic flow spatial average speed, traffic flow time average speed and traffic flow instantaneous speed. The definition method and characteristics of each type of traffic flow speed are shown below.

1) Spatial average speed. Spatial average speed refers to the calculation of the speed average of all vehicles in a specified section of the region or a section of the path, is a region or a section of the path as a unit for the calculation of the average speed, such as formula (1).

$$\bar{V} = \frac{S}{\frac{1}{N}\sum_{i=1}^{N} t_i} \tag{1}$$

In the formula S for the length of a road section; N for the total number of vehicles; t_i for the vehicle in the road section of the i th car traveling time, and the average of all vehicle time; $\bar{V}$ for the average spatial speed.

2) Time average speed. The time average speed is the average of the instantaneous speed of each vehicle through the specified cross-section calculated for a specified time range, as in Equation (2).

$$\bar{V} = \frac{1}{N}\sum_{i=1}^{N} v_i \tag{2}$$

In Eq. N is the total number of vehicles; v, is the instantaneous E velocity of a vehicle traveling to a cross section for the i rd vehicle in the section; and $\bar{V}$ is the time-averaged velocity.

3) Instantaneous speed. Instantaneous speed is the speed in terms of vehicles that describes the speed of a vehicle traveling to a certain cross-section.

2.1.2. Density. Traffic flow density is defined as the number of vehicles contained in a section of roadway per unit length at a given instant of time. It is calculated as in equation (3).

$$K = \frac{N}{L} \tag{3}$$

In the formula N is the number of all vehicles on a road section at a certain instant; L is the length of a road section; K is the density of traffic flow.

2.1.3. Possession. Vehicle occupancy has two components, time occupancy and space occupancy. The time occupancy rate is defined as the ratio of the time occupied by the vehicle passing through the detector to the total observation time in a certain observation time; the space occupancy rate is defined as the ratio of the total length of vehicles on a certain road section to the total length of the road section. The specific calculation formula is shown in (4).

1) Time occupancy

$$O_t = \frac{T_0}{T} \tag{4}$$

In Eq. (4) T_0 is the vehicle passage time through the detector; T is the total observation time; and O is the time occupancy rate.

2) Space occupancy

$$O_l = \frac{L_0}{L} \tag{5}$$

In Equation (5) L_0 is the total length of vehicles; L is the total length of the road section: O_l is the spatial occupancy.

3) Relationship between density and time occupancy

$$occ = l \times k \tag{6}$$

In Eq. (6) l is the sum of vehicle and detector lengths (taken as 6.7m); k is the density; and occ is the time occupancy.

Equation (6) is derived from equations (7) to (9), q is the flow rate, D is the length of the road section, N is the number of vehicles in the road section, u_s is the spatial average speed, and u_i is the time average speed. It can be seen through the formula that the relationship between time occupancy and density is linear, so according to formula (6), the mutual transformation of occupancy and density can be realized.

$$u_s = \frac{D}{\frac{1}{N}\sum_{i=1}^{N} t_i} = \frac{D}{\frac{1}{N}\sum_i \frac{D}{u_i}} = \frac{1}{\frac{1}{N}\sum_i \frac{1}{u_i}} \tag{7}$$

$$occ = \frac{\sum_i \frac{(l+d)}{u_i}}{T} = (l+d)\frac{N}{T}\frac{1}{N}\sum_i \frac{1}{u_i} \tag{8}$$

$$q = \frac{N}{T} = k \times u_s \tag{9}$$

2.1.4. Flow. Traffic flow volume is defined as the number of vehicles passing through a given cross-section of a roadway during the observation time.

$$q = \frac{N}{T} \tag{10}$$

In Equation (10) N is the number of vehicles passing through the cross-section during the observation time: T is the observation time; q is the traffic flow rate.

2.2. Pre-processing of traffic data

2.2.1. Handling of outliers, missing values, normalization:

1) Handling of outliers. The outlier judgment methods mainly include empirical method, box-and-line diagram method, normal distribution method and so on. Empirical method is a simple and convenient method, but there is too much subjectivity, it is based on historical experience, determine the range of parameter values, when more than this range of data is treated as an outlier, empirical method is mainly based on the conclusions of some historical research as the background for the determination of the range of parameter data. Box and line plot is a classic statistical data analysis, box and line plot is divided into box and line, box value includes information for the first quartile Q_1, median C, third quartile Q_3, the first quartile and third quartile is the data from the small to reach the order of the 25% and 75% of the value, the line value of the information includes the upper inner limit value and the lower inner limit value, the upper inner limit value of $Q_{up} = Q_3 + 1.5(Q_3 - Q_1)$, the lower inner limit value of $Q_{down} = Q_1 - 1.5(Q_3 - Q_1)$, the range of normal value The interval is $[Q_{down}, Q_{up}]$. The normal distribution method firstly requires that the distribution of the data obeys the normal distribution, when the distance from the mean value of 3 times the standard deviation of the data in the normal distribution curve is viewed as a small probability event, the probability value is less than 0.003, so when the distance of the data is more than 3 times the standard deviation of the data, the data can be considered as abnormal data, Fig. 1 shows the box-and-line diagram and the diagram of the normal distribution graph schematic diagram.

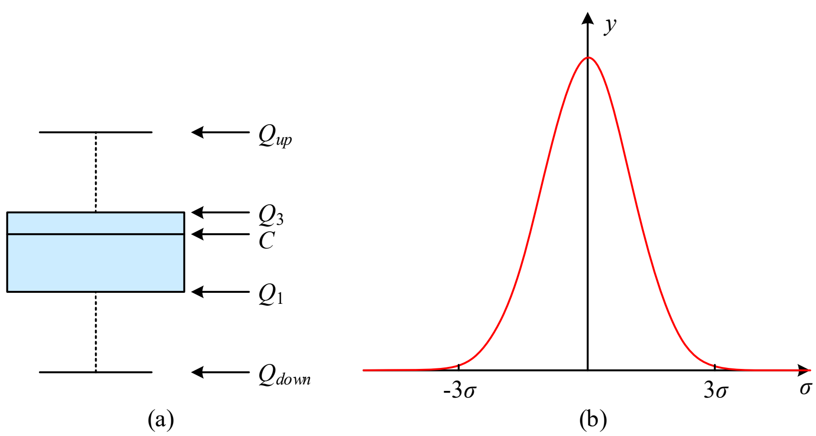

Fig. 1. Boxplot and a schematic diagram of the normal distribution

2) Missing value processing. Missing value processing methods mainly include discard method, historical value reference method, spline fitting interpolation method, etc. Discard method is the simplest missing value processing method, but it is easy to lose the key point data; historical value reference method is to refer to the data of the same time period in the history as the filler data of the current moment; spline fitting is a kind of interpolation method, which is classified into B-spline fitting and three-spline fitting, and the spline fitting can fill in the missing values by analyzing the values before and after the point to build an analytical function to depict the trend of the change before and after the point. Spline fitting fills in the missing values by analyzing the before and after values to establish an analytic function that depicts the trend before and after the point. Cubic spline fitting is shown in equation (11).

$$x(t) = A_0 + A_1 t + A_2 t^2 + A_3 t^3 \tag{11}$$

3) Normalization. The dimensionless processing of data has standardization and normalization processing, due to the standardization processing is related to the overall data variance and average value, suitable for the data transformation of more outliers and the data transformation of the output value range is not required: the normalization processing can be scaled to the data between the specified range, and the results are only related to the maximum and minimum values in the data, so the processing method is more sensitive to the outliers of the data. In this paper, there are fewer data outliers and missing values, and according to the needs of the prediction model, the data need to be scaled to the specified range, so this paper selects the normalization method to transform the data, such as shown in Equation (12) for scaling the data to [-1, 1], and shown in Equation (13) for scaling the data to between $[0,1]$.

$$x_{norm} = \frac{2 \times (x - x_{\min})}{x_{\max} - x_{\min}} - 1 \tag{12}$$

$$x_{norm} = \frac{x - x_{\min}}{x_{\max} - x_{\min}} \tag{13}$$

2.2.2. Data smoothing. Data smoothing can reduce the impact of data jitter on the prediction results, data filtering is the classic way of data smoothing and has better results.

FIR filter (Finite Impulse Response, FIR) is one of the classical digital filters, FIR filter can provide stable energy and phase information in the passband. FIR filtering of time series data can more accurately reflect the contour characteristics of the time series, so that in the subsequent time series prediction analysis can be more focused on the trend analysis of the time series, reducing the impact of transient noise on the results, thus improving the efficiency of data processing [26].

Since the data used in this study is characterized by strong randomness of instantaneous changes and is susceptible to the Gibbs effect (Gibs Effect), which makes it difficult to extract the frequency components and the spectral performance is more complex, this study chooses the Hanning window as the window function of the filter to perform low-pass filtering on the traffic data [27]. Hanning window is a kind of ascending cosine window, the decay speed of its spectrum is faster, which can effectively reduce the phenomenon of spectral leakage and boundary effect, and it is suitable for solving the signal with strong randomness and complex spectral characteristics. The Hanning window function is shown in Eq. (14), and the unit impulse response is shown in Eq. (15) and Eq. (16). Where N is the window length, k is the data point serial number, and F_c is the cutoff rate.

$$\omega(k) = 0.5 - 0.5\cos\left(\frac{2\pi k}{N-1}\right)\left(0 \le k \le \frac{N-1}{2}\right) \tag{14}$$

$$h(k) = h_d(k)\omega(k) \tag{15}$$

$$h_d(k) = \frac{\sin(2kF_c)}{\pi k} \tag{16}$$

2.3. Traffic flow prediction model based on spatio-temporal graph convolutional network

2.3.1. Modeling framework. The DDISTGCN model employs the design concept of spatio-temporal data fusion analysis to build a spatio-temporal map that captures the dynamic nature of traffic flow. This integrated framework not only provides sensitive insights into immediate changes in traffic flow, but also predicts potential trends in traffic flow, presenting the dependency of dynamically processing spatio-temporal information with predicted traffic flow. The specific structure of the model is shown in Fig. 2.

In the DDISTGCN model, the core structural unit is a series of cascading spatio-temporal blocks. Each spatio-temporal block contains graph convolutional layers that are specifically designed to process graph-structured data and learn spatial dependencies between nodes by utilizing adjacency matrices and node features. In the temporal dimension, these graph convolutional layers are able to track changes in node states over time, thus learning the dynamic patterns of traffic flow. The capture of this spatio-temporal correlation is crucial for predicting future traffic conditions, as it allows the model to not only mine current traffic flow patterns, but also predict future traffic flows based on historical data.

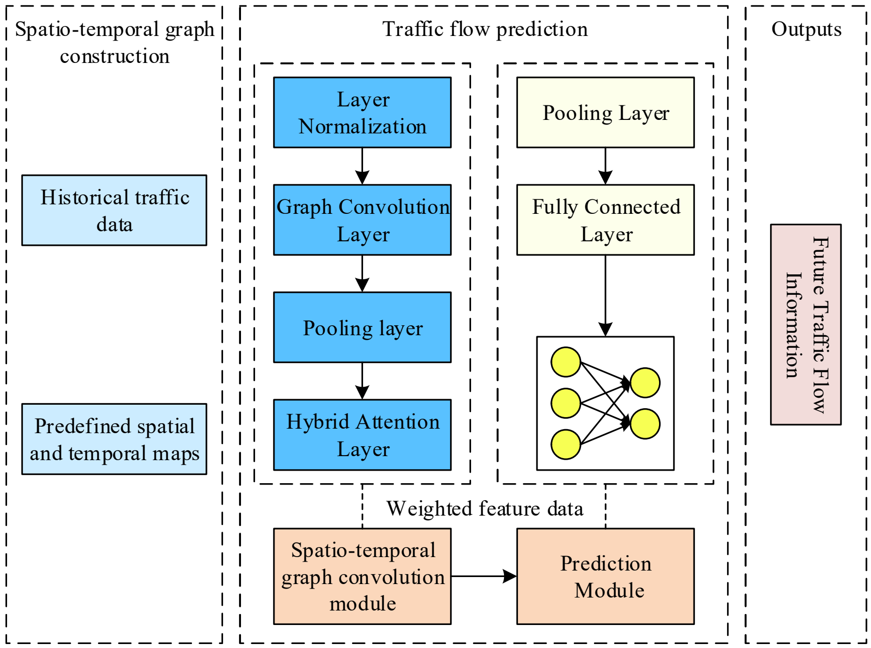

Fig. 2. Convolutional network model diagram of dynamic data interaction

The architectural focus of the DDISTGCN model can be summarized in three main components that form the core of its ability to predict traffic flows. The first is the construction of the spatio-temporal fusion map, which provides the model with a multi-dimensional data structure to accurately capture and analyze the spatio-temporal variations of traffic flows. Then, the important spatio-temporal features of traffic flow are convolved and captured by the spatio-temporal graph, embedded in the prediction module, and combined with the network node features to perform traffic flow prediction. This is followed by the hybrid attention layer, a mechanism that combines global and local perspectives, enabling the model to capture key traffic flow features at different time scales. Finally, there is the prediction module, which integrates the outputs of the first two components to achieve traffic flow prediction.

2.3.2. Spatio-temporal map convolution module. Since most of the other studies on road network traffic flow prediction rely on road structure information to construct predefined static maps, they are unable to characterize the dynamically changing temporal information of the road network. Therefore, in order to improve these problems, this thesis proposes a dynamic spatio-temporal graph convolution module based on fused spatio-temporal features.

In the framework of the DDISTGCN model, by constructing a spatio-temporal correlation graph and a spatial-temporal awareness graph, the model is able to provide a more accurate characterization of the dependencies between nodes. Nevertheless, the dynamic characterization of these dependencies needs to be further refined in order to cope with the challenges posed by changes in real-time traffic data. To address this need, the spatio-temporal graph convolution module designed in this chapter. This module combines spatio-temporal features to further enhance the model's ability to capture dynamic spatio-temporal dependencies. In addition, this mechanism enables a more accurate understanding of the dynamic relationships between nodes over time.

In order to fully utilize the spatio-temporal information and connect nodes with different time steps, a new hybrid spatio-temporal graph is proposed. As shown in Eq. (17), the adjacency matrix B of this graph is defined as:

$$B_{i,j} = e^{\left(-\frac{\left(\left(dist(v_1,v_2)(m+1)\right)^2\right)}{\sigma^2}\right)} \tag{17}$$

The associated edge weights of nodes v_1 and v_2 in a certain time step are defined in matrix B, where the weights of the edges are inversely proportional to the spatial distance. m in Eq. (18) represents the time difference. If $m = 0$, represents two nodes at the same moment in time, the formula can be expressed as:

$$B_{i,j} = e^{\left(-\frac{\left(dist(v_1,v_2)^2\right)}{\sigma^2}\right)} \tag{18}$$

In the model DDISTGCN presented in this thesis, an innovative perspective is adopted to explain and deal with dependencies in spatio-temporal data. Specifically, the model distinguishes between long-distance dependencies and short-distance dependencies, where long-distance dependencies represent global interactions, while short-distance dependencies are more concerned with local connections. This distinction is crucial for understanding and modeling dynamic spatio-temporal data, as the importance of information tends to vary at different time scales. In addition, the combination of long- and short-range information can provide unique insights. Therefore, the DDISTGCN model introduces a hybrid attention mechanism that efficiently integrates information from different time steps, selecting and aggregating information from key nodes through a designed attention score.

In this model, the hidden states of each node in different layers and time steps are precisely defined, and the attention score is computed based on these states to be able to capture the dynamic interactions between long and short distances. By first selecting node v_i at different locations and defining $x_i^{(n)} \in R^d$ as the hidden state of node v_i at the moment of time step t in layer n in this model, the attention score a_i^m can be expressed as:

$$a_i^m = \frac{e^{\varsigma_i^n}}{\sum_{n=1}^{N} e^{\varsigma_i^n}} \tag{19}$$

where ς_i^n is:

$$\varsigma_i^n = x_i^{(n)^T} B_i q \tag{20}$$

Then the attention fraction for long and short distances can be expressed as:

$$a_{i,j_1}^m = \frac{e^{\varsigma_{i,j_1}^n}}{\sum_{n=1}^{N} e^{\varsigma_{i,j_1}^n}} \tag{21}$$

where ς_{i,i_1}^n is:

$$\varsigma_{i,i_1}^n = x_i^{(n)^T} B_{i,i,1} q \tag{22}$$

where $B_{i,i_1} \in R^{d\times d}$, q are learnable parameters, N is the number of layers of the model, and a_i^m is the attention score computed with respect to $x_i^{(n)}$, whereby the hybrid attention mechanism can be represented as:

$$A_i = \frac{\sum\left(\hat{A}_{i,i_1} - \hat{A}_i\right)\left(\hat{A}_{i,i_2} - \hat{A}_i\right)}{\sqrt{\sum\left(\hat{A}_{i,i_1} - \hat{A}_i\right)^2}\sqrt{\sum\left(\hat{A}_{i,i_2} - \hat{A}_i\right)^2}} \tag{23}$$

where $\hat{A}_i$ and $\hat{A}_{i,j}$ are respectively:

$$\begin{aligned} \hat{A}_i &= \sum_{n=1}^{N} a_i^m x_i^{(n)} \\ \hat{A}_{i,i_1} &= \sum_{n=1}^{N} a_{i,i_1}^m x_i^{(n)} \end{aligned} \tag{24}$$

2.3.3. Forecasting module. In the DDISTGCN model, a hybrid attention mechanism is introduced to efficiently integrate information across different time steps to optimize the performance of the prediction module. The prediction module, followed by the pooling layer, is one of the core components of the model.

In order to quantify the prediction accuracy and guide the model training process, the model is designed with a composite loss function based on MAE and RSME, aiming to minimize the discrepancy between the prediction results and the real data.RMSE and MAE, as the two main error assessment criteria, each possesses its own unique strengths and limitations.RMSE is extremely sensitive to the outliers in the data, which can help to identify and emphasize the impacts; while MAE provides a way to perform equal optimization on all predicted values, resulting in a model with stable performance across a wide range of applications. Specifically, the loss function of this model is Eq. (25), where $\propto$ is used to balance the loss of MAE and RMSE.

$$L' = \frac{1}{C}\left(\sum_{i=1}^{c}\left(\left|\tilde{A}_{t+i} - A_{t+i}\right| + \propto \frac{\left|\tilde{A}_{t+i} - A_{t+i}\right|}{A_{t+i}}\right)\right) \tag{25}$$

3. Path selection game based on traffic flow prediction

3.1. Description of the evolutionary game problem

3.1.1. Description of Evolutionary Game Relationships. Only after the manager decides to implement the information guidance strategy based on the traffic flow prediction, the traveler can make the next path choice decision, i.e., whether to listen to the guidance information to adjust their own path to travel, otherwise, the traveler does not have to make the choice of whether to listen to the guidance information command. The evolutionary game relationship between the manager and the traveler in the two stages is shown in Figure 3.

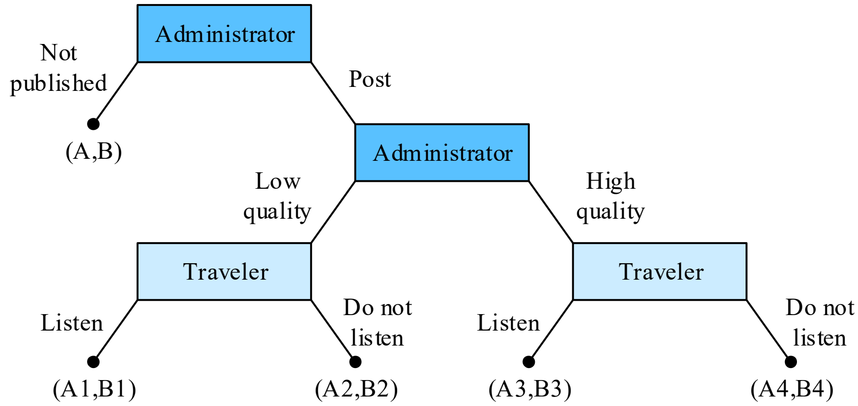

Fig. 3. A schematic diagram of the two-stage game relationship guided by information

3.1.2. Basic assumptions of the evolutionary game. Considering the characteristics of the game problem in traffic management and the content of the study, this paper makes the following assumptions:

1) Game subject assumption. It is assumed that there are only two participants in the evolutionary game process, i.e., the asymmetric game of traffic managers and traffic travelers.

2) Finite rationality assumption. Both game participants to meet the requirements of the assumption of finite rationality, in the pursuit of maximizing their own interests at the same time and can not be completely accurate measure of their own interests.

3) Game order hypothesis. The game between the manager and the traveler is not a one-time decision, there is a dynamic process of change, after copying and learning to reach the stable state of the game. At the same time, transportation managers have the right to make decisions in the first stage, i.e., managers decide to implement the information guidance strategy or not to implement the information guidance strategy first. Only after the manager decides to implement the information guidance strategy, the game can enter the second stage.

3.2. Evolutionary game modeling

3.2.1. A two-stage evolutionary game model. The game decision is made when both sides of the game make choices in their respective decision sets. Suppose the probability that the manager chooses not to release any guidance information is x, then the probability that he chooses to release guidance information is $1-x$. Meanwhile, after deciding to release guidance information, the probability that he chooses to release high-quality information is y, and $1-y$ is the probability that he chooses to release low-quality guidance information. Assuming that the probability that the traveler listens to the guidance information is z, the probability that he/she does not listen to the guidance information is $1-z(x,y,z\in[0,1])$. To summarize, the payment matrix of the two-stage game between the manager and the traveler is shown in Figure 4.

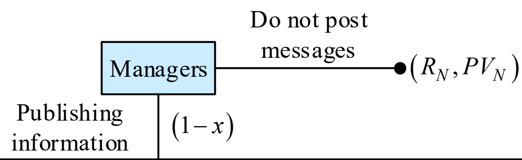

Manager	Traveler	
	Follow the guide (z)	Not following the guidance (1-z)
High-quality information (y)	$\left(R_N + R_H + P_H - C_H^G, PV_{HF} + B - C_H^T\right)$	$\left(R_N + V - C_H^G, PV_N + B - C_H^T\right)$
Low-quality information (1-y)	$\left(R_N + R_L + P_L - C_L^G, PV_{LF} + B - C_L^T\right)$	$\left(R_N + V - C_L^G, PV_N + B - C_L^T\right)$

Fig. 4. Two-stage evolutionary game payment matrix of managers and travelers

3.2.2. Replication dynamics of evolutionary games. Differences in the magnitude of benefits under different decisions cause the game between the manager and the traveler to evolve to different stable equilibria. Considering the manager's choice preference, two directions of evolution are considered: Direction 1, the manager does not release guidance information and the game process ends in the first stage; Direction 2, the manager releases guidance information but needs to determine whether to release high-quality or low-quality guidance information based on the response of the travelers.

Direction 1: The manager does not release guidance information.

Regardless of whether or not the traveler follows the information guidance, there is a situation in which the manager chooses not to publish the guidance information when the benefits of publishing either high or low quality guidance information are lower than the benefits of not publishing the guidance information. In this case, there is a relationship between the decision gains: $R_H + P_H < C_H^G$ and $R_L + P_L < C_L^G$.

Because the manager has the power to prioritize decisions in the game with the traveler, as long as the manager's gain from not releasing guidance is higher than the gain from releasing information, the manager will make the decision of not releasing information, resulting in the game between the two stopping in the first stage. At this point, the traveler does not need to make the decision to follow or not follow the information guidance, so the result of the stabilization game under Direction 1 is $\left(R_N, PV_N\right)$.

Direction 2: The manager releases guidance information.

When $V > C_H^G$ or $V > C_L^G$, the benefits of the manager issuing high-quality guidance information or issuing low-quality guidance information are both Direction 2: The manager issues guidance information.

When $V > C_H^G$ or $V > C_L^G$, the manager's gain from releasing high-quality guidance information or releasing low-quality guidance information is higher than the gain from not releasing guidance information, at which point it can be determined $x = 0$. The two-stage evolutionary game in Fig. 4 can be simplified into an 2×2 asymmetric game as shown in Table 1.

Table 1. Evolutionary game payment matrix between managers and travelers direction 2

Manager	Out of the walker	
	Follow the boot (z)	Unguided $(1-z)$
High quality information (y)	$\left(R_N+R_H+P_H-C_H^G, PV_{HF}+B-C_H^T\right)$	$\left(R_N+V-C_H^G, PV_N+B-C_H^T\right)$
Low quality information $(1-y)$	$\left(R_N+R_L+P_L-C_L^G, PV_{LF}+B-C_L^T\right)$	$\left(R_N+V-C_L^G, PV_N+B-C_L^T\right)$

Let W_H^G and W_L^G denote the expected payoffs for managers who choose to publish high-quality information and publish low-quality guidance information, respectively, and W^G denote the average expected payoff for managers. According to the payment function in Table 1, it can be obtained:

$$W_H^G = z\left(R_N+R_H+P_H-C_H^G\right)+(1-z)\left(R_N+V-C_H^G\right) \tag{26}$$

$$W_L^G = z\left(R_N+R_L+P_L-C_L^G\right)+(1-z)\left(R_0+V-C_L^G\right) \tag{27}$$

$$W^G = y\cdot W_H^G+(1-y)\cdot W_L^G \tag{28}$$

If $W_H^G > W^G$, the manager's benefit from choosing the strategy of publishing high-quality guidance information is greater than the average benefit, and over time, as long as the manager has basic judgment and observation, sooner or later he or she will be able to find out that publishing high-quality guidance information is a better choice of decision, and thus adjust the choice of information guidance strategy to make his or her own benefit higher, and so the probability of choosing the strategy of publishing high-quality guidance information will increase; on the contrary, if $W_L^G > W^G$. In sum. The replicated dynamic equation of managers' choice of publishing high-quality guidance information strategy evolves in a determined direction:

$$\begin{aligned}\tilde{W}^G &= y\left(W_H^G-W^G\right)=y(1-y)\left(W_H^G-W_L^G\right)\\ &= y(1-y)\Big[z\Big(R_H-R_L+b\cdot\left(PV_{HF}-PV_N\right)-b\cdot\left(PV_{LF}-PV_N\right)\Big)\\ &-C_H^G+C_L^G\Big]\end{aligned} \tag{29}$$

where $b\left(PV_{HF}-PV_N\right)-b\left(PV_{LF}-PV_N\right)$ is equivalent to the relative gain in perceived reference value under high quality guidance versus low quality guidance, i.e., $b\left(PV_{HF}-PV_{LF}\right)$. Similarly, by substituting R_{HF} and R_{LF} into the above equation and letting ΔPV and ΔT denote the relative difference between high and low quality, the replication dynamics equation for the manager's strategy of releasing high-quality guidance messages can be expressed in equation (30).

$$\tilde{W}^G = y(1-y)\left[z(a\Delta T+b\Delta PV)-C_H^G+C_L^G\right] \tag{30}$$

Similarly, it can be obtained by letting W_F^T and W_{NF}^T denote the expected returns of the travelers choosing to listen to and not listen to the information guidance, respectively, and W^T denote the average expected return of the travelers:

$$W_{NF}^T = y\left(PV_N+B-C_H^T\right)+(1-y)\left(PV_N+B-C_L^T\right) \tag{31}$$

$$W^T = z\cdot W_F^T+(1-z)\cdot W_{NF}^T \tag{32}$$

$$W^T = z\cdot W_F^T+(1-z)\cdot W_{NF}^T \tag{33}$$

In summary, the replicated dynamic equations for the traveler's choice to listen to the information-guided strategy also evolve in a defined direction:

$$\begin{aligned}\tilde{W}^T &= z\left(W_F^T - W^T\right) = z(1-z)\left(W_F^T - W_{NF}^T\right) \\ &= z(1-z)\left[y\left(PV_{HF} - PV_{LF}\right) + PV_{LF} - PV_N\right] \\ &= z(1-z)\left[y\Delta PV + \Delta PV_L\right]\end{aligned} \tag{34}$$

3.3. Evolutionary stability analysis

Under Direction 1, the game between the two parties stops at the first stage, so there is no need for a stability analysis; only the situation in Direction 2 needs to be analyzed. First, the replicated dynamic equations for the manager and the traveler are analyzed. For the manager's dynamic equation, if $z = \frac{c_H^G - c_L^G}{a\Delta T + b\Delta PV}$, then $\tilde{W}^G$ stays constant at 0 and all y are in a steady state; if $z \neq \frac{c_G^G - c_L^G}{a\Delta T + b\Delta PV}$, then both $y=0$ and $y=1$ are in a steady state. For the traveler's dynamic equation, if $y = -\frac{\Delta PV_L}{\Delta PV}$, then $\tilde{W}^T$ is held constant at 0 and all z are in steady state; if $y \neq -\frac{\Delta PV_L}{\Delta PV}$, at this point $z=0$ and $z=1$ are in steady state. The phase diagram in Figure 5 reflects the replicated dynamic relationship and stability of the manager and the traveler. Therefore, Let $\tilde{W}^G = \frac{dy}{dt} = 0$ and $\tilde{W}^T = \frac{dz}{dt} = 0$ get the five local equilibrium points of the replication dynamics in Direction 2, which are $A=(0,0)$, $B=(0,1)$, $C=(1,0)$, $D=(1,1)$, and $E = \left(-\frac{\Delta PV_L}{\Delta PV}, \frac{C_H^G - C_L^G}{a\Delta T + b\Delta PV}\right)$. The stability of the local equilibrium points is analyzed using the Jacobi matrix judgment method proposed by Friedman. The local stability of the equilibrium points is analyzed based on the Jacobi matrix of the dynamic replication system to obtain the evolutionary stabilization strategy formed by the two-stage evolutionary game between the manager and the traveler.

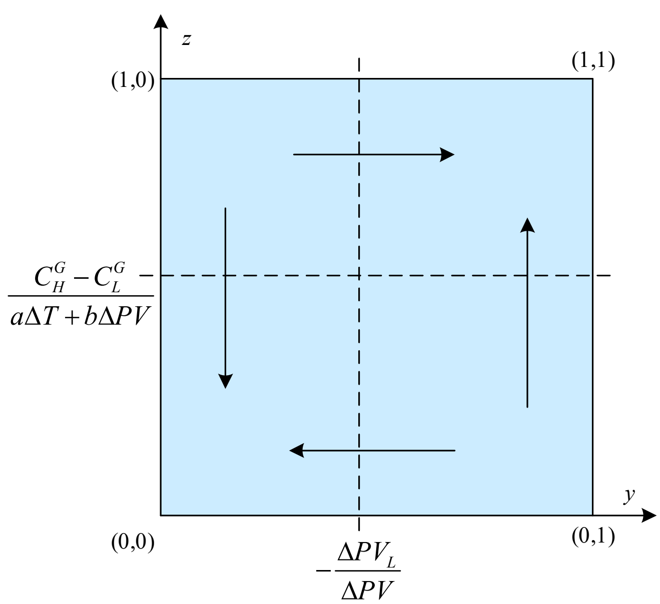

Fig. 5. Copy dynamic relationship and stability between managers and travelers

Substituting the five local equilibria into the Jacobi matrix yields the specific values taken at each equilibrium, as shown in Table 2.

Table 2. Local stability point characteristics of the evolution game in direction 2

Equilibrium point	Determinant	Trace
A	$\left(C_L^G - C_H^G\right)\Delta PV_L$	$C_L^G - C_H^G + \Delta PV_L$
B	$-\Delta PV_L\left(a\Delta T + b\Delta PV - C_H^G + C_L^G\right)$	$a\Delta T + b\Delta PV - C_H^G + C_L^G - \Delta PV_L$
C	$\Delta PV_H\left(C_H^G - C_L^G\right)$	$C_H^G - C_L^G + \Delta PV_H$
C	$-\Delta PV_H\left[C_H^G - C_L^G - (a\Delta T + b\Delta PV)\right]$	$C_H^G - C_L^G - (a\Delta T + b\Delta PV) - \Delta PV_H$
E	E^*	0

where $E^* = \dfrac{\Delta PV_L\left(\Delta PV + \Delta PV_L\right)\left(C_H^G - C_L^G\right)\left(a\Delta T + b\Delta PV - c_H^G + C_L^G\right)}{\Delta PV(a\Delta T + b\Delta PV)}$.

Since the local equilibrium point E corresponds to a trace of the Jacobi matrix of 0, E is not an evolutionarily stable strategy for the game. Discuss whether the other four local equilibrium points are evolutionarily stable by integrating the two stages. Denoting the choice probabilities of the manager and the traveler as $S(x, y, z)$, the integrated strategy combinations are: $S_1(1,-,-)$, $S_2(0,0,0)$, $S_3(0,0,1)$, $S_4(0,1,0)$, and $S_5(0,1,1)$.

4. Route selection based on traffic simulation models

4.1. *Traffic flow prediction simulation analysis*

4.1.1. Simulation environment and parameter selection. The experimental conditions for the model in this chapter: the CPU is Intel(R) Core(TM) i5-10200H, the operating system is Windows 10, the graphics card is NVIDIA GeForce GTX 1650, and the processing framework for the data flow graph is the Tensorflow1.16.0 framework based on Python3.7.0.

The parameters were selected as shown in Table 3, and the learning rate of the model in this chapter was set to 0.001, the batch size was 64, the number of iterations was 1000, the L2 loss function was used, 80% of the data was used as the training set, and the Adam optimization algorithm was used for the training of the model.

Table 3. Parameter selection

Parameter type	Parameter value
Learning rate	0.001
Batch size	64
epoch	1000
Loss function	L2 loss function
Optimization algorithm	Adam optimization algorithm
The number of hidden layers of neurons	128

The number of hidden layer neurons is related to the complexity and expressive ability of the model, and choosing the appropriate number of hidden layer neurons in the model construction is very critical for model performance improvement. For the model in this paper, when the number of hidden layer neurons is [16, 32, 64, 100, 128], the results are shown in Figure 6. From the results, it can be seen that as the number of hidden neurons gradually rises, the coefficient of determination and accuracy of the model prediction of the test set gradually rises, while the two errors are reduced, when the number of neurons in the hidden layer is greater than 64, the various performance indicators tend to stabilize, and when the neurons are 128 the performance of the various performance reaches its highest. Therefore, for the model in this paper, the number of neurons in the hidden layer is set to 128.

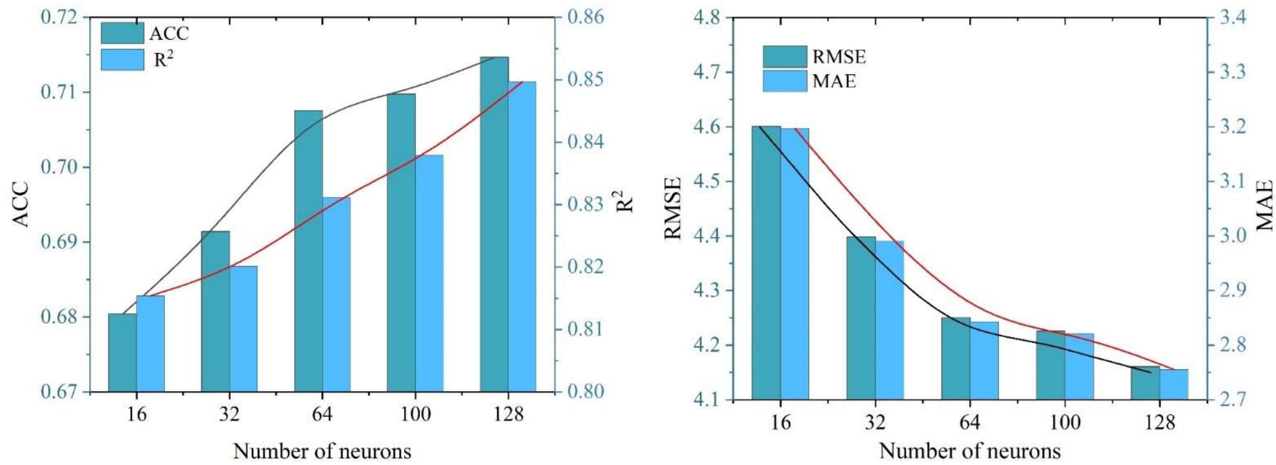

(a) Evaluation (b) Units

Fig. 6. Predictive performance affects the experimental results

In deep learning, an epoch is a complete iteration of the entire training dataset. In each epoch, the neural network updates the weights and biases once. By increasing the number of epochs, the model can be made to learn the features in the dataset more fully and improve the model performance. However, if there are too many epochs, it may lead to overfitting. Therefore, an appropriate number of iterations needs to be chosen.

For the model in this chapter, when the number of iterations were [600, 1000, 1500, 2000, 2500, 3000], the results of each performance index are shown in Figure 7, we can see that when the number of iterations more than 1000 predicted that the various performance indicators tend to stabilize, so taking into account the performance and training time in this paper, the model selects the number of iterations of 1000 times.

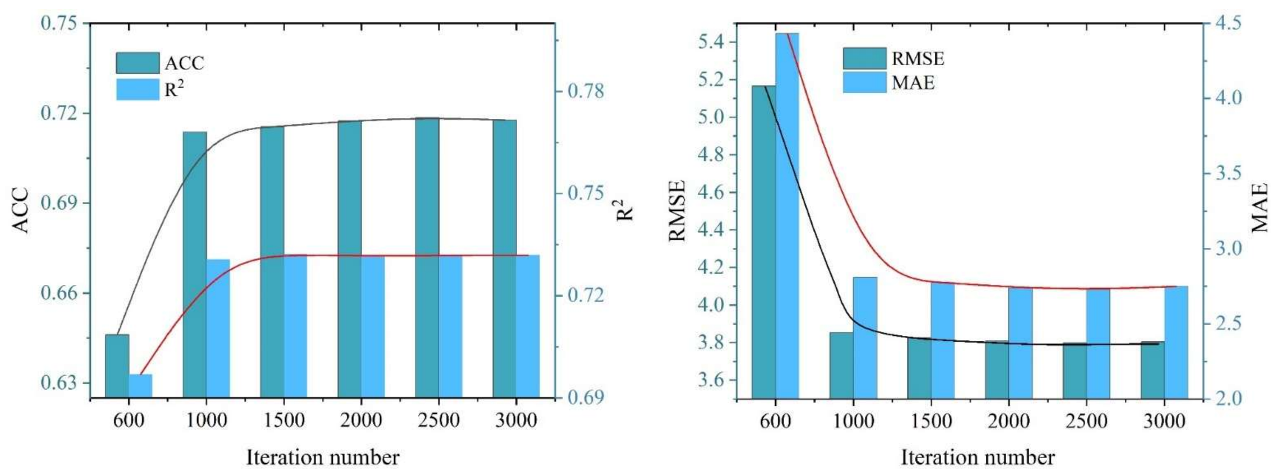

(a) Evaluation (b) Epoch

Fig. 7. The number of iterations on the prediction performance affects the experimental results

4.1.2. Experimental results and analysis. Fig. 8 shows the result graph of single-step prediction of a road section on the test set in the experiment, and the results of a two-day period are selected for visualization, from which it can be seen that the overall trend of the predicted values and the real values are roughly the same, and the predicted curves fit the actual curves better. However, at the peak and valley values, there is a large deviation between the predicted values and the real values, which may be due to the fact that the data at the peak and valley values are more complicated and unstable, and there are many factors affecting the prediction accuracy; in addition, the training data of the model may not be able to completely cover these complicated situations, which also affects the prediction effect of the model.

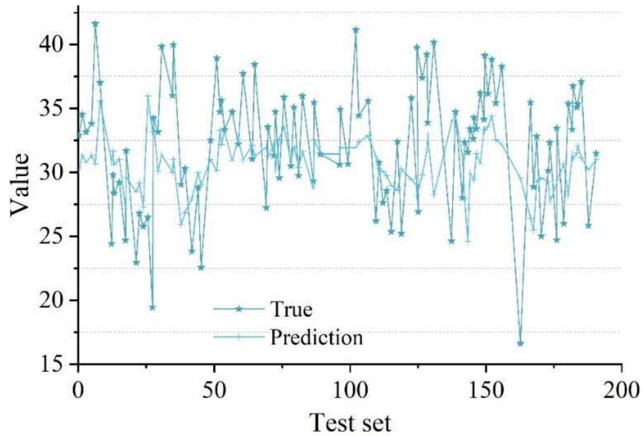

Fig. 8. Results of prediction

The experiments in this chapter utilize data from the past 10 time steps for prediction, and the model prediction results when the prediction step is 15min are shown in Table 4.

On the experimental dataset in this chapter, compared with the traditional statistical methods (e.g., ARIMA), the DFTGCN model has a stronger prediction ability, with a substantial improvement in the three metrics of RMSE, MAE, and ACC, which are optimized by 40.24%, 41.60%, and 89.12%, respectively, which may be attributed to the limitation of the traditional methods in dealing with this kind of data with a high level of complexity, the cannot capture the nonlinear trends in the data.

In addition compared to the AST-GCN model, which has the second best effect, the effect is improved in the four indicators of RMSE, MAE, ACC and R^2, which are optimized by at least 1.51%, 1.64%, 0.39% and 0.34%, respectively, which may be attributed to the fact that the AST-GCN model simply splices the external information with the traffic data in the treatment of external information and fails to pay attention to the connection, while the model in this chapter captures the spatial and temporal characteristics of external information through time domain feature embedding and space domain feature embedding, and thus is able to improve the prediction performance of the model.

Overall the DDISTGCN model has certain advantages in the traffic prediction problem, which can better capture the spatio-temporal relationship between the data and the influence of external factors on the traffic, so as to improve the prediction accuracy and precision.

Table 4. Contrasts the performance indicators between different models at predicting 15min

Model	RMSE	MAE	ACC	R^2
SVR	4.217	2.801	0.756	0.887
ARIMA	6.862	4.721	0.423	*
HA	5.848	3.752	0.73	0.851
GRU	4.186	2.785	0.757	0.888
T-GCN	4.165	2.826	0.759	0.891
AST-GCN	4.164	2.803	0.76	0.891
DDISTGCN	4.101	2.757	0.763	0.894

4.2. Traffic Route Selection Analysis Based on Traffic Flow Prediction

4.2.1. Analysis of evolutionary results. The evolutionary game model is based on the two assumptions that the travelers have high finite rationality and heterogeneity. Therefore, according to the obedience rate of the travelers to the static AITS information, the travelers are divided into three categories, and the evolution process and results of each path are analyzed by taking the path adjustment rate γ_m as 1/t, and the perceptual error parameter θ_1 of each category of travelers (the positive reciprocal of the perceptual error, $\theta_3 < \theta_2 < \theta_1$) as 1.5, 1, and 0.6 for example, respectively.

Figure 9 shows the evolution process of each pathway flow, and the following conclusions can be clearly drawn: the fastest converging pathway is path 2, which takes 8 days, followed by path 1 and path 6, which take 16 days, and path 4, which takes 27 days, and the slower converging paths are path 3 and path 5, which take 37 days; each pathway flow changes significantly before the 10th day, and there is only a small amount of change after that. Therefore, the model as a whole converges slightly faster than the replicated dynamic evolutionary game model under low-rational groups.

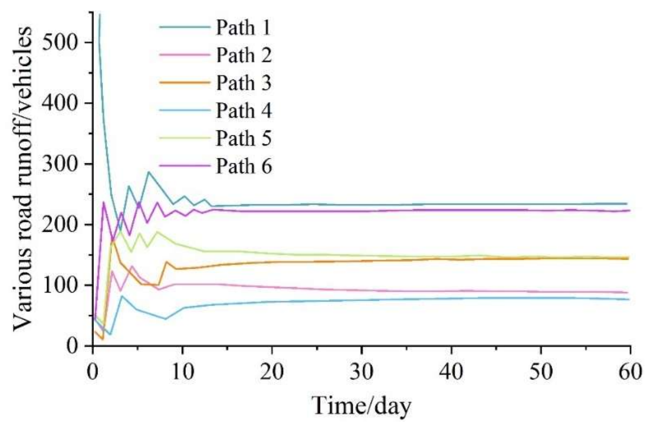

Fig. 9. Flow evolution process of each path

Table 5 shows the flow rate, travel time and cumulative outlook for each path in reaching equilibrium. It is evident that the travel time for each path is approximately equal at 57.90 minutes and the cumulative outlook values are all negative, which indicates that the traveler cannot find a path with a positive cumulative outlook, making it impossible for the flow of any path to suddenly increase or decrease. The travel times for Path 1 and Path 6 are small, 57.67 and 57.71 minutes, respectively, and the travel times for Path 2 and Path 4 are relatively large, 58.31 and 58.35 minutes, respectively, and the difference between the maximum and minimum values is 0.71. In contrast, the traffic volume of path 1 and path 6 is larger, respectively 231 and 221 vehicles, and the traffic volume of path 2 and path 4 is smaller, respectively 93 and 74 vehicles. The comparison of path flow and path time shows that travelers with higher rationality are more sensitive to the changes of travel time and cumulative prospect value of each path, and are more inclined to make choices that are beneficial to their own interests, and the cumulative prospect value of the equilibrium state is all negative, which also reflects that the travelers aim at pursuing the largest positive cumulative prospect value.

Table 5. Properties of each path under the evolutionary equilibrium

Path	Path flow/vehicle	Path time/min.	Cumulative prospect
1	231.54	57.67	-2.67
2	93.67	58.31	-3.61
3	138.14	57.89	-3.08
4	74.22	58.35	-3.65
5	148.27	57.91	-3.14

6	221.12	57.71	-2.7

4.2.2. Analysis of route adjustment rates. In this paper, the flow evolution process of path 3 is analyzed as an example based on taking different fixed and variable values of γ_m.

Fig. 10 shows the evolution results for path 3 taking fixed values such as γ_m= 0.05, 0.1, 0.2 and variable values such as $\gamma_m = \gamma_m/2$, γ_m=1/t, respectively. In particular, the initial value of γ_m in $\gamma_m = \gamma_m/2$ is 1. First of all, when γ_m takes a fixed value, the convergence speed of the flow of path 3 is accelerated with the decrease of two, and the fluctuation amplitude of the flow decreases with the decrease of two; and when γ_m=1/t, the flow of path 3 fluctuates with a larger amplitude, and the convergence speed of it is faster than that of the convergence speed of γ_m=0.1, 0.2, and slower than that of the convergence speed of γ_m=0.05; The evolutionary dynamic model under higher rationality and the replicated dynamic model under lower rationality have both differences and common points. Evolutionary dynamic model under higher rationality and the replicated dynamic model under lower rationality have differences and common points: the same is that when the value of & is larger, the fluctuation of the path flow will be very obvious; the difference is that when the value of & is gradually converging to 1, the path with decreasing flow will gradually evolve to the state of zero flow, and in the replicated dynamic model, it will result in the flow of the path in the future evolution is still in the state of zero flow, which will make the flow of some paths increase significantly and thus This will cause the flow of some paths to increase dramatically and exceed the capacity limit, which does not happen in the two-stage evolutionary game model with long-term dynamics between the manager and the travelers, but it will cause the flow of the paths to keep fluctuating in a small range, which shows that the value of γ_m should not be taken as large as it should be.

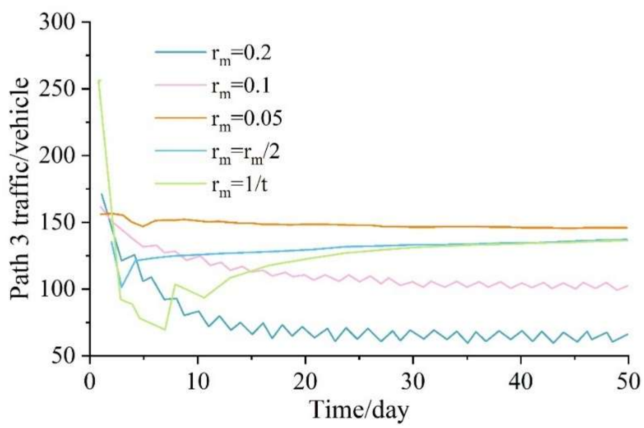

Fig. 10. Path 3 shows the flow curve changes at different values of r_m

4.2.3. Analysis of the volume of traveler transfers. Scenarios 1 and 2 belong to the manager's perspective, and scenario 3 belongs to the traveler's own perspective. Scenario 1 includes the transfers M2.1 and M2.3 of the second type of travelers to the first and third categories, M3.1 and M3.2 of the third type of travelers to the first and second categories, respectively, Scenario 2 only considers the transfer volume between the second and third types of travelers from M2.3 and M3.2, and the transfer of the third type of travelers to the first category M3.1, and the third scenario is the perspective of the travelers, which considers the error and magnitude of the first three days on the basis of the transfer relationship of the second category $m_{i,j}$ and different perception times of various types of travelers. Therefore, this part takes the change curve of the number of first-class travelers as the main research objective, and analyzes it through three scenarios.

Figure 11 shows the evolution of the number of Type 1 travelers in the three scenarios. It can be clearly seen from the figure that the evolution curves of the number of the first type of travelers in Case 1 and Case 2 under the manager's perspective are relatively close to each other, due to the fact that Case 1 has taken more consideration of the direct transfer of the second type of travelers to the first type of travelers compared to Case 2, which makes a difference between the two in the initial time of the transfer and the amount of the transfer. In contrast, the difference between Case 3 and Case 3 from the perspective of the travelers themselves is larger, because at the beginning of the evolution, the flow rate of certain paths will increase significantly, causing the formation of congestion on these paths, which leads to excessive travel time. Also, since scenario 3 is calculated by the perceived time of each of the three types of travelers, whereas the first two scenarios are calculated by the overall average travel time difference, the perceived time difference between the first type of travelers and the third type of travelers in scenario 3 is amplified, making the sum of the perceived time differences of the first three days in day 5 of the calculation example larger, to have the solid dotted curves as shown in the graph on the day when there is a large shift of the third type of travelers to the the first type of travelers.

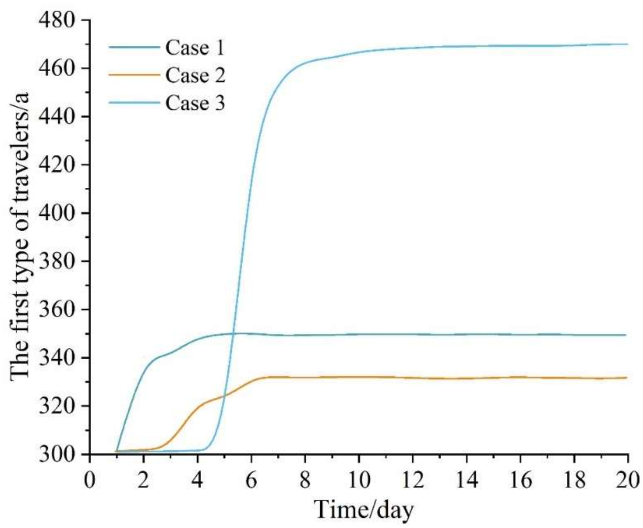

Fig. 11. Number curve change of type 1 travelers in three cases

5. Recommendations for traffic congestion management countermeasures based on traffic flow forecasts

1) Enhancing the ability to study and judge road traffic conditions. Accurate understanding of the current road traffic system is the basis for the road traffic department to release relevant traffic information. Travelers based on road conditions, travel routes suggested information to choose, prompting the traffic system to form a new distribution of traffic flow so as to achieve the purpose of changing the state of the traffic system. Therefore, in order to reasonably guide the public travel, the traffic management department should first strengthen the research and judgment of the road traffic condition.

Make full use of the Internet of Things and the Internet of vehicles, big data, distributed computing, artificial intelligence and other modern information processing technologies, analyze and process the huge amount of data collected by the information collection equipment, and at the same time excavate the potential information hidden in the data, make a comprehensive study and judgment of the traffic condition of the road traffic system, and provide the travelers with accurate and reasonable information about the road traffic capacity and the travel routes suggested to guide the travelers to make appropriate road choice decisions, so as to balance the road traffic condition and to improve the traffic conditions. It provides travelers with accurate and reasonable information on road capacity and travel route suggestions, guides travelers to make appropriate decisions on road selection, thus balancing the distribution of traffic flow in the road network, reducing the occurrence of traffic congestion or enhancing the capacity of congested road sections.

2) Strengthen the construction of information system hardware equipment to provide protection for information collection. First of all, the hardware equipment of the information system which is already backward and cannot adapt to the requirements of modern traffic management should be updated in time to improve the efficiency of information collection. For example, at this stage, the video monitoring equipment which can transmit the real-time traffic operation situation has been widely used in each city road network system, and the original traffic monitoring equipment which can only record the traffic operation situation of the road network and upload the historical information can not adapt to the demand of the traffic management due to the disadvantages of delayed information and limited information storing capacity, therefore, this kind of equipment should be eliminated and replaced with the video monitoring equipment which can transmit the real-time road situation in a timely manner. Therefore, such equipment should be eliminated and replaced with video monitoring equipment that can transmit real-time road conditions in a timely manner.

3) Compare the actual and expected results of congestion management and adjust the information dissemination strategy in time. Based on the real-time data of travelers' actual choices and traffic flow distribution under the effect of information, the actual effect of using information to manage congestion will be compared with the expected results, and the information dissemination strategy will be adjusted in a timely manner according to the different differences between the actual effect and the expected results.

Adjustment of the information release strategy by the traffic management department is mainly realized by changing the characteristics of information release, including adjusting the time of information release, the content of information release, the way of information release, and choosing the appropriate information release channels. Based on the adjustment of the information release strategy, it affects the behavior of the travelers, so that the traffic flow in the road network system can be redistributed again, so that the actual effect of traffic congestion management is closer to the expected effect.

6. Conclusion

The study proposes a deep learning algorithm based on fused spatio-temporal graphical convolutional networks for traffic state prediction (DDISTGCN) and uses evolutionary game theory to analyze the effectiveness of information guidance policies implemented by traffic managers in realistic scenarios. The main conclusions of the article are as follows:

1) A real traffic dataset is used to validate the performance of the model, and the results show that the DDISTGCN model has higher accuracy and better robustness than other existing traffic flow prediction methods.

2) As the path adjustment rate γ_m decreases, the path flow converges faster. And the flow evolution curve when γ_m =1/t is more realistic. The perception error parameter θ_1 for the first type of travelers cannot be taken too large, and the path convergence speed is faster.

References

[1] Aleksandr, N., Vladimir, Z., & Anastasiya, F. (2018). Dynamic traffic re-routing as a method of reducing the congestion level of road network elements. Journal of applied engineering science, 16(1).

[2] Zhang, L., Zeng, G., Li, D., Huang, H. J., Stanley, H. E., & Havlin, S. (2019). Scale-free resilience of real traffic jams. Proceedings of the National Academy of Sciences, 116(18), 8673-8678.

[3] Yue, W., Li, C., Mao, G., Cheng, N., & Zhou, D. (2021). Evolution of road traffic congestion control: A survey from perspective of sensing, communication, and computation. China Communications, 18(12), 151-177.

[4] Almatar, K. M. (2023). Traffic congestion patterns in the urban road network:(Dammam metropolitan area). Ain Shams engineering journal, 14(3), 101886.

[5] Jabbarpour, M. R., Zarrabi, H., Khokhar, R. H., Shamshirband, S., & Choo, K. K. R. (2018). Applications of computational intelligence in vehicle traffic congestion problem: a survey. Soft Computing, 22, 2299-2320.

[6] Qi, L., Zhou, M., & Luan, W. (2018). A dynamic road incident information delivery strategy to reduce urban traffic congestion. IEEE/CAA Journal of Automatica Sinica, 5(5), 934-945.

[7] Xu, X., Chen, A., Jansuwan, S., Yang, C., & Ryu, S. (2018). Transportation network redundancy: Complementary measures and computational methods. Transportation Research Part B: Methodological, 114, 68-85.

[8] Huang, F., Xu, J., & Weng, J. (2020). Multi-task travel route planning with a flexible deep learning framework. IEEE Transactions on Intelligent Transportation Systems, 22(7), 3907-3918.

[9] Wang, D., Zhang, J., Cao, W., Li, J., & Zheng, Y. (2018, April). When will you arrive? Estimating travel time based on deep neural networks. In Proceedings of the AAAI conference on artificial intelligence (Vol. 32, No. 1).

[10] Polson, N. G., & Sokolov, V. O. (2017). Deep learning for short-term traffic flow prediction. Transportation Research Part C: Emerging Technologies, 79, 1-17.

[11] Petersen, N. C., Rodrigues, F., & Pereira, F. C. (2019). Multi-output bus travel time prediction with convolutional LSTM neural network. Expert Systems with Applications, 120, 426-435.

[12] James, J. Q., Yu, W., & Gu, J. (2019). Online vehicle routing with neural combinatorial optimization and deep reinforcement learning. IEEE Transactions on Intelligent Transportation Systems, 20(10), 3806-3817.

[13] Law, R., Li, G., Fong, D. K. C., & Han, X. (2019). Tourism demand forecasting: A deep learning approach. Annals of tourism research, 75, 410-423.

[14] Cheng, L., Chen, X., De Vos, J., Lai, X., & Witlox, F. (2019). Applying a random forest method approach to model travel mode choice behavior. Travel behaviour and society, 14, 1-10.

[15] Kandasamy, K., Neiswanger, W., Schneider, J., Poczos, B., & Xing, E. P. (2018). Neural architecture search with bayesian optimisation and optimal transport. Advances in neural information processing systems, 31.

[16] Cheng, Z., Pang, M. S., & Pavlou, P. A. (2020). Mitigating traffic congestion: The role of intelligent transportation systems. Information Systems Research, 31(3), 653-674.

[17] Bliemer, M. C., Raadsen, M. P., Brederode, L. J., Bell, M. G., Wismans, L. J., & Smith, M. J. (2017). Genetics of traffic assignment models for strategic transport planning. Transport reviews, 37(1), 56-78.

[18] Sadollah, A., Gao, K., Zhang, Y., Zhang, Y., & Su, R. (2019). Management of traffic congestion in adaptive traffic signals using a novel classification-based approach. Engineering Optimization, 51(9), 1509-1528.

[19] Wu, N., Li, D., & Xi, Y. (2018). Distributed weighted balanced control of traffic signals for urban traffic congestion. IEEE transactions on intelligent transportation systems, 20(10), 3710-3720.

[20] Zhang, X., Guan, H., Zhu, H., & Zhu, J. (2019). Analysis of travel mode choice behavior considering the indifference threshold. Sustainability, 11(19), 5495.

[21] Zhang, X., & Guan, H. (2019). Research on travel mode choice behaviors based on evolutionary game model considering the indifference threshold. IEEE Access, 7, 174083-174091.

[22] Di, X., Liu, H. X., Zhu, S., & Levinson, D. M. (2017). Indifference bands for boundedly rational route switching. Transportation, 44, 1169-1194.

[23] Menelaou, C., Timotheou, S., Kolios, P., Panayiotou, C. G., & Polycarpou, M. M. (2018). Minimizing traffic congestion through continuous-time route reservations with travel time predictions. IEEE Transactions on Intelligent Vehicles, 4(1), 141-153.

[24] Shafiei, S., Gu, Z., & Saberi, M. (2018). Calibration and validation of a simulation-based dynamic traffic assignment model for a large-scale congested network. Simulation Modelling Practice and Theory, 86, 169-186.

[25] Saeedmanesh, M., & Geroliminis, N. (2017). Dynamic clustering and propagation of congestion in heterogeneously congested urban traffic networks. Transportation research procedia, 23, 962-979.

[26] Krzysztof Jaskólski,Wojciech Czaplinski & Arkadiusz Tomczak. (2024). Spectral Analysis of Compass Errors Based on Fast Fourier Transform and Reduction Absolute Errors Using a Pass-Band Finite Impulse Response Filter. Polish Maritime Research(2),109-120.

[27] Poggiali Davide,Cecchin Diego,Campi Cristina & De Marchi Stefano. (2021). Oversampling Errors in Multimodal Medical Imaging Are Due to the Gibbs Effect. Mathematics(12),1348-1348.